Journal of Sound and Vibration (2001) **243**(1), 117–125
doi:10.1006/jsvi.2000.3394, available online at http://www.idealibrary.com on IDEAL®

NON-LINEAR VIBRATION ANALYSIS AND SUBHARMONIC WHIRL FREQUENCIES OF THE JEFFCOTT ROTOR MODEL

H. DIKEN

Mechanical Engineering Department, King Abdulaziz University, P.O. Box: 80204, *Jeddah* 21589, *Saudi Arabia*

(*Received* 3 *June* 1999, *and in final form* 12 *September* 2000)

In this analysis, a Jeffcott rotor model is used which is a thin disk located on a flexible shaft which is simply supported at the ends. The non-linear dynamic equations of the rotor are obtained. A perturbation technique is used to obtain approximate linear equations for the non-linear equations. The non-linear equations and approximate linear equations are solved numerically and the solutions compared. The approximate linear equations correctly predict the non-linear vibration. It has been experimentally observed in many researches that in addition to the synchronous whirl, there exist subharmonic vibrations which may cause instability. This is generally attributed to the dry friction, non-linear or asymmetric stiffness, rubs, fluid-film bearing clearances. This study shows that there exist two subharmonic transient vibrations caused by the non-linearity of the system itself. The two subharmonic frequencies are equal to $(\omega + \omega_n)$ and $(\omega - \omega_n)$ and also the supersynchronous component of the vibration becomes unstable when the speed ratio ω/ω_n is $\geqslant 2$.

1. INTRODUCTION

In general, the equations developed for the Jeffcott rotor model are non-linear but after assuming synchronous whirl, the steady state equations become simple and linear and have a well-known solution. This solution shows that resonance occurs when the rotational speed is equal to the critical speed (natural frequency) of the system. Constant whirl amplitude and phase angle can be calculated as a function of damping and speed ratio [1, 2, 3]. Ehrich [4] first noticed and analyzed the appearance of a pseudo-critical peak in the response amplitude for a rotating machine operating at twice its fundamental critical rotational speed. The frequency of vibration was at the fundamental natural frequency, that is, at exactly $\frac{1}{2}$ the operating speed. He referred to the phenomena as subharmonic vibration. Bently [5] did systematic experimental work on the second and third order responses of an experimental rotor, observing pseudo-critical peaks at respectively twice the fundamental critical speed with $\frac{1}{2}$ per revolution frequency, and at three times fundamental critical speed with $\frac{1}{3}$ per revolution frequency. Childs [6] analyzed the problem, expanding on Bently's modelling of the problem, and referred to the problem as fractional frequency rotor motion. Ehrich [7] states that rotor dynamic instabilities and self-excited vibrations generally take the form of lateral flexural vibrations at the rotor natural or critical frequency different from, and most often below the running speed. The "subsynchronous", or "super-critical" vibration amplitude generally increases so sharply with increasing running speed or power that, if the vibration is monitored, additional increases in running speed are deemed impossible, or if the vibration is not monitored, the equipment is damaged severely or

0022-460X/01/210117 + 09 $35.00/0

destroyed. This class of phenomena imposes a continuing restraint on the performance capabilities of rotating machinery, and continues to cause difficulties in the design and operation of high-performance machinery [8]. Ehrich [7] has modelled the rotor with the planar asymmetry in the stator stiffness and shown that asymmetric stiffness may cause the subharmonic and superharmonic resonance peaks. Lund [9] states that critical speed calculations (which ignores damping and presupposes isotropic bearings and, therefore, circular whirl orbits) are performed as a calculation of the resonant frequencies of a beam in planar lateral vibrations when actually the shaft itself only bends and does not vibrate at all. Thus, for a whirl motion at frequency ω as observed by stationary probes, a strain gauge attached to the shaft will register a vibration with frequency components $(\omega + \omega_n)$ and $(\omega - \omega_n)$. Subsynchronous whirl is also experimentally observed in the work of Khan *et al.* [10]. Ehrich [11] and Childs [3] attribute this subsynchronous whirl to dry friction, rubs, trapped fluid, hysteresis or rotor internal damping, oil seals and uneven journal clearances in the fluid-film bearings. Ganesan [12] recently studied the effect of non-symmetric clearances in bearings.

In this study a Jeffcott model of rotor dynamics is used. The non-linear equations of the system are obtained and solved numerically without making a synchronous whirl assumption. A perturbation technique is used and the non-linear equations are approximated by a set of linear differential equations. The first part of the differential equations give the synchronous whirl and phase angle, the second part of the differential equations produces a characteristic equation which gives two frequencies equal to $(\omega + \omega_n)$ and $(\omega - \omega_n)$. The study shows that on top of the synchronous whirl and the steady state whirl radius there is one subsynchronous and one supersynchronous damped transient vibration resulting directly from the non-linear dynamics of the motion itself and the supersynchronous component becomes unstable when the speed ratio (frequency ratio) ω/ω_n is equal or greater than two.

2. ANALYSIS

Figure 1 shows the Jeffcott rotor model which is a thin unbalanced disk located at the middle of a flexible shaft which is simply supported by two bearings at the ends. Here O is the center of the disc before deflection. S is the geometric center of the disk which coincides with O before deflection. G is the mass center of the disk. r is the deflection of the shaft, e is the mass eccentricity, θ is the whirl angle, ω is the spin of the disk. The governing equations in the radial and tangential directions are obtained as follows [1, 2, 3]

$$\ddot{r} + 2\zeta\omega_n\dot{r} + (\omega_n^2 - \dot{\theta}^2)r = e\omega^2\cos(\omega t - \theta),$$

$$r\ddot{\theta} + (2\zeta\omega_n r + 2\dot{r})\dot{\theta} = e\omega^2\sin(\omega t - \theta). \tag{1}$$

Here r is the whirl radius, ζ the damping ratio, ω_n the natural frequency of the rotor, θ the whirl angle, e the mass eccentricity, and ω the rotational speed which is assumed constant. After defining a new whirl radius and a new non-dimensional time, the non-linear differential equations will take the form

$$\eta'' + 2\zeta p\eta' + (p^2 - \theta'^2)\eta = \cos(\tau - \theta),$$

$$\eta\theta'' + (2\zeta p\eta + 2\eta')\theta' = \sin(\tau - \theta), \tag{2}$$

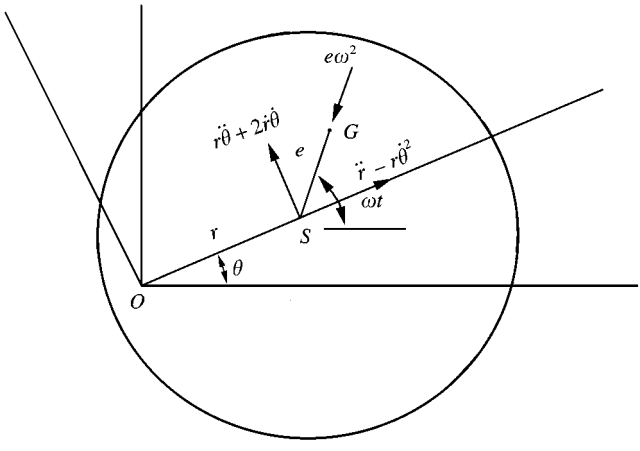

Figure 1. Jeffcott rotor model.

where

$$\eta = \frac{r}{e}, \quad p = \frac{\omega_n}{\omega}, \quad \tau = \omega t, \qquad (.)' = \frac{\mathrm{d}}{\mathrm{d}\tau} = \frac{1}{\omega}\frac{\mathrm{d}}{\mathrm{d}t}.$$

Here η is the non-dimensional whirl radius, ζ the damping ratio, p the speed ratio (frequency ratio), and τ the non-dimensional time. In these equations derivatives are with respect to the non-dimensional time τ and indicated by a prime notation. Now an approximate solution to the problem of the following type is assumed:

$$\eta(\tau) = \eta_0(\tau) + \mu\eta_1(\tau) + \cdots,$$
$$\theta(\tau) = \theta_0(\tau) + \mu\theta_1(\tau) + \cdots. \tag{3}$$

Here μ is the perturbation parameter. After putting the assumed solution into equation (2) and neglecting higher order terms of μ, the following set of differential equations are obtained:

$$\begin{pmatrix} \eta_0'' + 2\zeta p\eta_0' + (p^2 - \theta_0'^2)\eta_0 = \cos(\tau - \theta_0) \\ \eta_0\theta_0'' + (2\zeta p\eta_0 + 2\eta_0')\theta_0' = \sin(\tau - \theta_0) \end{pmatrix} \tag{4}$$
$$+ \mu\begin{pmatrix} \eta_1'' + 2\zeta p\eta_1' + (p^2 - \theta_0'^2)\eta_1 - 2\theta_0'\eta_0\theta_1' - \theta_1\sin(\tau - \theta_0) = 0 \\ \eta_0\theta_1'' + (2\zeta p\eta_0 + 2\eta_0')\theta_1' + 2\theta_0'\eta_1' + (\theta_0'' + 2\zeta p\theta_0')\eta_1 + \theta_1\cos(\tau - \theta_0) = 0 \end{pmatrix} + \cdots.$$

For the first part of the equations of equation (4) synchronous whirl is assumed which means that at steady state the whirl speed is constant and equal to rotational speed, and the whirl radius r is also constant, this means $\omega = \dot{\theta}$, $\ddot{\theta} = \ddot{r} = \dot{r} = 0$. In terms of the non-dimensional parameters these conditions are $\theta_0' = 1$, $\theta_0'' = \eta_0'' = \eta_0' = 0$. After these assumptions equation (1) is reduced to

$$(\omega_n^2 - \dot{\theta}^2)r = e\omega^2\cos\psi,$$
$$2\zeta\omega_n r\dot{\theta} = e\omega^2\sin\psi. \tag{5}$$

Here $\psi = \omega t - \theta$ is the phase angle. In non-dimensional form, equation (5) is

$$(p^2 - \theta'^2)\eta = \cos\psi,$$

$$2\zeta p\eta\theta' = \sin\psi. \tag{6}$$

From equation (5) the solution for whirl radius r and phase angle ψ can be found as

$$r = \frac{e(\omega/\omega_n)^2}{\sqrt{[1-(\omega/\omega_n)^2]^2 + [2\zeta\,\omega/\omega_n]^2}}, \qquad \psi = (\omega t - \theta) = \tan^{-1}\frac{2\zeta\,\omega/\omega_n}{1-(\omega/\omega_n)^2}. \tag{7}$$

In non-dimensional form equation (7) is

$$\eta_0 = \frac{1}{\sqrt{(p^2-1)^2 + (2\zeta p)^2}}, \qquad \psi = \tau - \theta_0 = \tan^{-1}\frac{2\zeta p}{p^2-1}. \tag{8}$$

Equation (8) is also a solution for equation (6). For a given p and ζ, η_0 and ψ are constant. If one puts these values into the second part of equation (4), they will become a linear set of differential equations which is

$$\begin{bmatrix} 1 & 0 \\ 0 & \eta_0 \end{bmatrix}\begin{bmatrix} \eta_1'' \\ \theta_1'' \end{bmatrix} + \begin{bmatrix} 2\zeta p & -2\eta_0 \\ 2 & 2\zeta p\eta_0 \end{bmatrix}\begin{bmatrix} \eta_1' \\ \theta_1' \end{bmatrix} + \begin{bmatrix} (p^2-1) & -\sin\psi \\ 2\zeta p & \cos\psi \end{bmatrix}\begin{bmatrix} \eta_1 \\ \theta_1 \end{bmatrix} = \begin{bmatrix} 0 \\ 0 \end{bmatrix}. \tag{9}$$

When this equation is solved, $\eta_1(\tau)$ and $\theta_1(\tau)$ are obtained and together with the solution given in equation (8) an approximate solution will be obtained. The non-linear equations given by equation (2) are solved using a Runga–Kutta method. The equations given by equation (9) are also solved with the same numerical method and according to equation (3) an approximate solution is obtained and the results are compared. The plots are shown in Figures 2–5. The approximate solution is plotted with dashed lines and shifted with the

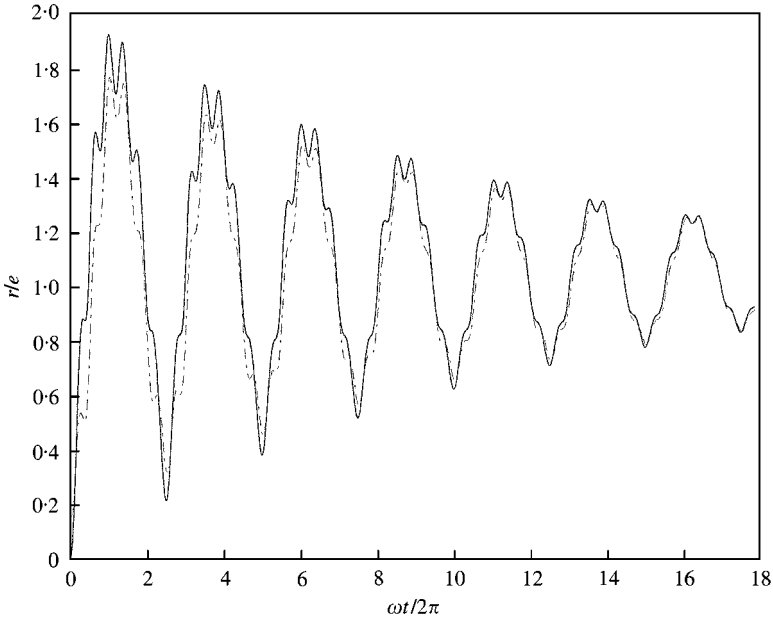

Figure 2. Whirl radius for the subcritical case $\zeta = 0{\cdot}01$, $p = 1{\cdot}4$, $\mu = 88{\cdot}48$: —, non-linear, –·–·– linearized.

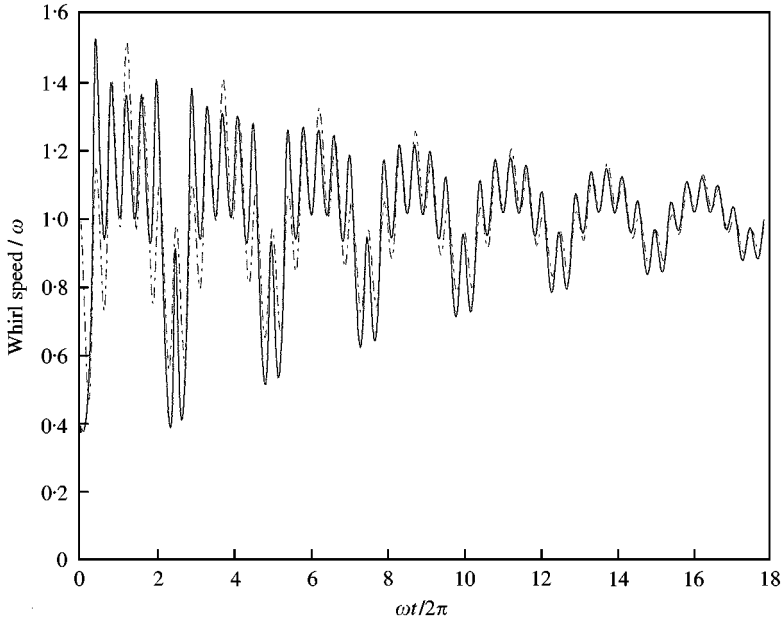

Figure 3. Whirl speed for the subcritical case $\zeta = 0{\cdot}01$, $p = 1{\cdot}4$, $\mu = 88{\cdot}48$: —, non-linear, – · – · – linearized.

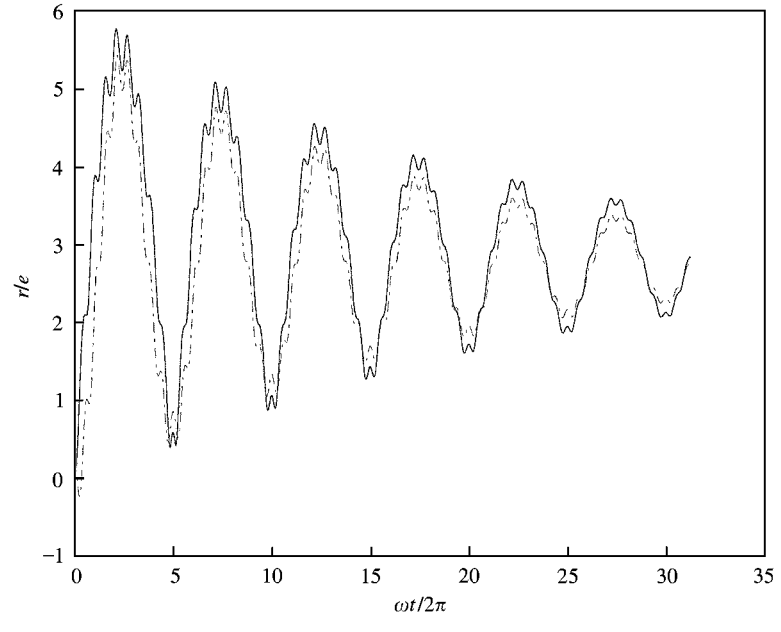

Figure 4. Whirl radius for the super-critical case $\zeta = 0{\cdot}01$, $p = 0{\cdot}8$, $\mu = 256{\cdot}32$: —, non-linear, – · – · – linearized.

amount of phase angle ψ to match with the actual solutions. Figures 2 and 3 show the results for the subcritical speed $p = 1{\cdot}4$ and for the damping $\zeta = 0{\cdot}01$. Figures 4 and 5 show the results for the supercritical speed $p = 0{\cdot}8$ and for the damping $\zeta = 0{\cdot}01$. As can be seen from the plots approximate solution matches well with the solution of the non-linear

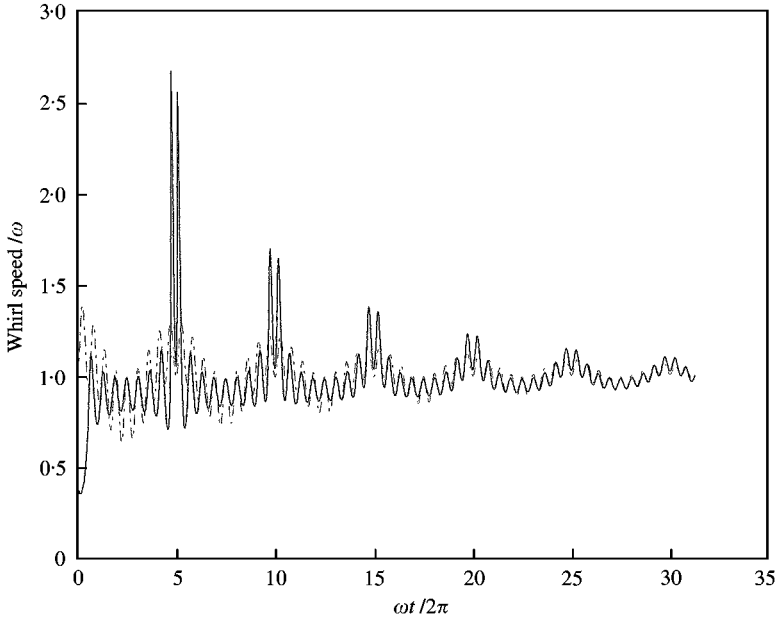

Figure 5. Whirl radius for super-critical case $\zeta = 0{\cdot}01$, $p = 0{\cdot}8$, $\mu = 256{\cdot}32$: —, non-linear, – · – · – linearized.

TABLE 1

The roots of the characteristic equation for $\zeta = 0{\cdot}01$

$p = \omega_n/\omega$	ω/ω_n	$s_{1,2}$	$\zeta_{1,2}$	$\omega_{1,2}/\omega$
0·4	2·5	0·0035 ± 1·39j	0·0025	1·4
		− 0·0115 ± 0·59j	0·0192	0·6
0·5	2·0	0·00 ± 1·5j	0·00	1·5
		− 0·01 ± 0·49j	0·02	0·5
0·8	1·25	− 0·0068 ± 1·79j	0·0038	1·8
		− 0·0092 ± 0·19j	0·0462	0·2
1·0	1·0	− 0·01 ± 1·99j	0·005	2
		− 0·01 ± 0·00j	1	0
1·25	0·8	− 0·0135 ± 2·24j	0·006	2·25
		− 0·0115 ± 0·24j	0·046	0·25
2·0	0·5	− 0·0225 ± 2·99j	0·0075	3
		− 0·0175 ± 0·99j	0·0175	1
2·5	0·4	− 0·028 ± 3·49j	0·008	3·5
		− 0·022 ± 1·49j	0·0147	1·5

equations. The results indicate that on top of synchronous whirl radius and synchronous whirl speed there are two damped oscillations, one is weakly damped the other one is strongly damped. These damped frequencies can be obtained from the characteristic equation of the equation (9):

$$\eta_0 s^4 + 4\zeta p\eta_0 s^3 + (4\zeta^2 p^2\eta_0 + p^2\eta_0 + 3\eta_0 + \cos\psi)s^2$$

$$+ 2(\zeta p^3\eta_0 + \zeta p\eta_0 + \zeta p\cos\psi + \sin\psi)s + (p^2 - 1)\cos\psi + 2\zeta p\sin\psi = 0. \qquad (10)$$

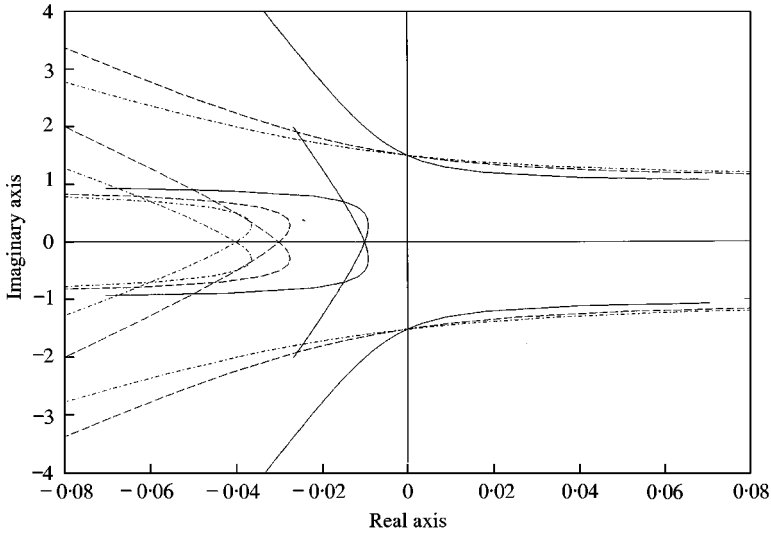

Figure 6. Root locus of the subharmonic frequencies. Solid line $\zeta = 0{\cdot}01$, dashed line $\zeta = 0{\cdot}03$, dash-dot line $\zeta = 0{\cdot}05$.

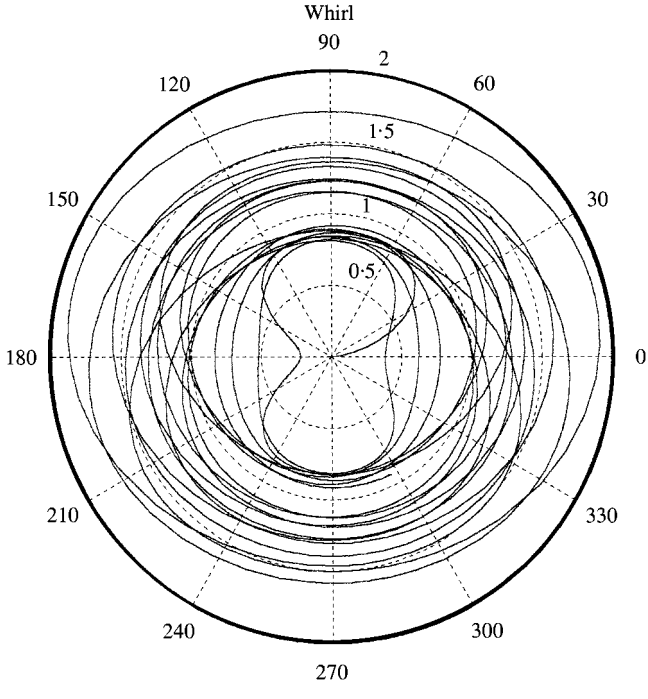

Figure 7. Polar plot of the whirl radius of the non-linear solution for the subcritical speed, $\zeta = 0{\cdot}01$, $p = 1{\cdot}4$.

Some of the roots of this characteristic equation are tabulated in Table 1.

In this table the first column shows the speed ratio $p = \omega_n/\omega$, the second column is the inverse of p which is ω/ω_n, in the third column are the roots of the characteristic equation given by equation (10). The roots indicate two damped vibrations, corresponding damping ratios $\zeta_{1,2}$ and natural frequencies $\omega_{1,2}$ which are given in the fourth and fifth columns.

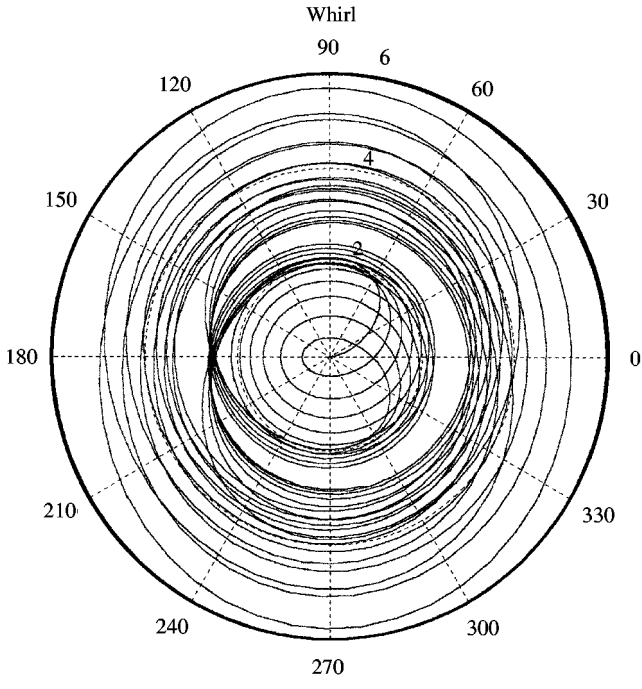

Figure 8. Polar plot of the whirl radius of the non-linear solution for the super-critical speed, $\zeta = 0{\cdot}01$, $p = 0{\cdot}8$.

These values are calculated according to the formulae

$$s_1 = -\omega_1\zeta_1 \pm (\omega_1\sqrt{\zeta_1^2 - 1})j,$$

$$s_2 = -\omega_2\zeta_2 \pm (\omega_2\sqrt{\zeta_2^2 - 1})j. \tag{11}$$

The roots indicate that there are two subfrequencies which are equal to $p_{1,2} = p \pm 1$, in other words $\omega_{1,2} = \omega_n \pm \omega$. Another observation is such that when $p \leqslant 0{\cdot}5$ or $\omega/\omega_n \geqslant 2$, one of the roots has positive real part which means that system is unstable. If the system is running with super-critical speed at which the ratio is equal to two or greater, the superharmonic vibration amplitudes will grow rapidly and cause instability. The rootlocus of the characteristic equation is shown in Figure 6. It is clear from the plot that for $p \leqslant 0{\cdot}5$ one root which gives the superharmonic frequency, has positive real part. At $p = 0{\cdot}5$ the rootlocus crosses the imaginary axis. This crossing point is not changed for different ζ. In Figures 7 and 8 polar plots of whirl radius are shown which are obtained from the solution of the non-linear equations. Figure 7 shows the whirl for the subcritical speed. Since the subharmonic components are damping quickly, the whirling approaches to a steady circle but in Figure 8 which shows the whirl for the super-critical speed, the subharmonic components are weakly damped, which is why they are effective and whirl motion does not approach to steady circle but has a kind of whipping or wobbling.

This analysis explains the reasons of the subharmonic vibrations observed in some experimental works. The non-linear behavior of the rotor itself has a constant whirl radius and synchronous whirl speed plus subharmonic and superharmonic vibrations. For the speed ratios greater than or equal to two, the superharmonic frequency component has a positive real part which causes instability.

3. CONCLUSION

In this study, a Jeffcott rotor model is assumed for the analysis which is a thin unbalanced disk mounted on a flexible shaft and simply supported by bearings at the ends. The non-linear dynamic equations of the system are obtained and solved numerically. A perturbation technique is used to approximate the non-linear equation and two sets of linear differential equations are obtained. The first set of equations gives the well-known steady state synchronous whirl radius and constant phase angle. The second set of equations is a linear set of second order damped vibration equations which has two frequencies which are $\omega_1 = (\omega + \omega_n)$ and $\omega_2 = (\omega - \omega_n)$. The solution of the approximate equations also matches well the solution of the non-linear equations. In previous works, the subharmonic frequencies are assumed to be caused by hysteresis, dry friction, rubs, bearing clearance and non-linear or asymmetric stiffness. This analysis shows that subsynchronous and supersynchronous frequencies which are frequently observed in experiments, may be caused by the non-linear dynamics of the rotor itself.

REFERENCES

1. W. T. THOMSON 1981 *Theory of Vibration with Applications*. Englewood Cliffs, NJ: Prentice Hall.
2. C. W. LEE 1993 *Vibration Analysis of Rotors* Dordrecht: Kluwer Academic Publishers.
3. D. CHILDS 1993 *Turbomachinery Rotordynamics*. New York: John Wiley and Sons.
4. F. F. EHRICH 1966 *American Society of Mechanical Engineers Journal of Engineering for Power* **88**, 56–65. Subharmonic vibration of rotors in bearing clearance.
5. D. E. BENTLY 1974 *American Society of Mechanical Engineers Journal of Engineering for Power* **96**, 60–71. Forced subrotative speed dynamic action of rotating machinery.
6. D. W. CHILDS 1982 *American Society of Mechanical Engineers Journal of Engineering for Power* **104**, 533–541. Fractional frequency rotor motion due to nonsymmetric clearance effects.
7. F. F. EHRICH 1988 *American Society of Mechanical Engineers Journal of Vibration, Acoustics, Stress and Reliability in Design* **110**, 9–16. High order subharmonic response of high speed rotors in bearing clearance.
8. F. F. EHRICH 1988 *Proceedings of the Second International Symposium on Transport Phenomena, Dynamics, and Design of Rotating Machinery* Part II, Hemisphere Pub. Co., 1990, 3–25. A state of the art survey in rotordynamics—nonlinear and self excited vibration phenomena.
9. J. W. LUND 1988 *Proceedings of the Second International Symposium on Transport Phenomena, Dynamics, and Design of Rotating Machinery* 27–33. Topics in Rotor Dynamics.
10. A. F. KHAN, M. K. GHAURI, R. H. SHAH, E. A. MUKHTAR, A. HUSSAIN and M. A. ATTA 1996 *Proceedings of the 1st National Conference on Vibrations in Rotating Machinery, Islamabad, Pakistan*, 527–534. A case study of subsynchronous whirl in a flexible rotor system.
11. F. F. EHRICH 1992 *Handbook of Rotordynamics* New York: McGraw-Hill.
12. R. GANESAN 1997 *American Society of Mechanical Engineers Journal of Engineering for Gas Turbines and Power* **119**, 418–424. Nonlinear vibrations and stability of a rotor-bearing system with nonsymmetric clearances.

APPENDIX A: NOMENCLATURE

r	whirl radius or deflection of the geometric center S
ζ	damping ratio of the flexible shaft and disk system
ω_n	natural frequency or critical speed
ω	rotational speed
e	mass eccentricity
η	non-dimensional whirl radius (r/e)
p	speed ratio or frequency ratio (ω_n/ω)
τ	non-dimensional time (ωt)
$\theta, \dot{\theta}$	whirl angle and whirl speed
θ', θ''	first and second derivative with respect to the non-dimensional time τ